Dr. Pankaj Malik, 2026, 14:4
ISSN (Online): 2348-4098
ISSN (Print): 2395-4752

International Journal of Science, Engineering and Technology
An Open Access Journal

Vehicle-Specific Underbody Collision Prediction Using Vision, Vehicle Dynamics, and Physics-Guided Machine Learning

[1]Dr. Pankaj Malik, [2]Yash Upadhyay, [3]Swaraj Singh Rajput, [4]Anuj Patidar, [5]Taher Fakhri
[1,2,3,4,5]Computer Science Engineering, Medicaps University, Indore, India

Abstract- Underbody collision is a vehicle-specific safety problem encountered while traversing potholes, speed breakers, road humps, deep depressions, rocks, and uneven or off-road surfaces. Conventional vision-based advanced driver assistance systems (ADAS) can detect road anomalies, but anomaly detection alone does not determine whether a particular vehicle will experience underbody contact. This paper presents an Intelligent Vehicle-Specific Underbody Collision Prediction (IV-UCP) framework that integrates forward-camera road-obstacle detection, road-geometry estimation, vehicle geometry, vehicle dynamics, and a physics-guided minimum-clearance model. The framework represents road geometry, vehicle characteristics, and dynamic state in a multimodal feature vector and uses machine learning to estimate collision probability and risk level. A conservative safe-speed module, cross-vehicle evaluation protocol, ablation analysis, explainable AI, and real-time deployment evaluation are also incorporated. The physical criterion C_min = min_x[Z_u(x)-Z_r(x)] is used as an interpretable clearance feature, while uncertainty and ground-truth quality are treated as important experimental considerations. The numerical values currently retained in the manuscript are explicitly identified as tentative or target values where verified experimental measurements are not available; they must be replaced by measured results before making empirical performance claims. The framework therefore provides a structured path from road-anomaly recognition to vehicle-specific underbody collision-risk prediction and driver assistance.

Keywords— Underbody Collision Prediction, Ground Clearance, Road Geometry, Vehicle Dynamics, Computer Vision, Machine Learning, Physics-Guided Machine Learning, ADAS, Pothole Detection, Speed-Breaker Detection, Safe-Speed Prediction, Explainable AI.

I. INTRODUCTION

Road-surface irregularities are a persistent challenge for vehicle safety, ride comfort, and vehicle durability. Potholes, speed breakers, road humps, deep depressions, stones, uneven road transitions, and off-road terrain can impose large dynamic loads on vehicles and may cause direct contact between the road and vehicle underbody.

Recent developments in computer vision and deep learning have enabled vehicles to detect potholes, speed breakers, road objects, and other road anomalies using cameras and deep neural networks. Such systems provide valuable information to drivers and autonomous vehicles. However, identifying a road anomaly is fundamentally different from determining whether the anomaly represents a collision threat to a particular vehicle.

For example, consider two vehicles approaching the same speed breaker. A vehicle with 190 mm ground clearance may safely traverse the obstacle, whereas a vehicle with 125 mm clearance may experience underbody contact. Even for the same vehicle, the risk can change with vehicle speed because suspension compression, longitudinal acceleration, and pitch alter the effective clearance.

Therefore, underbody collision should be modeled as a vehicle-road interaction problem:

$$P(\text{Collision})=f\,(\text{Road, Vehicle, Dynamics})$$

rather than as a simple road-object detection problem:

$$P(\text{Collision})=f(\text{Road})$$

This paper proposes an intelligent framework that integrates visual road perception with vehicle-specific geometry and dynamic state.

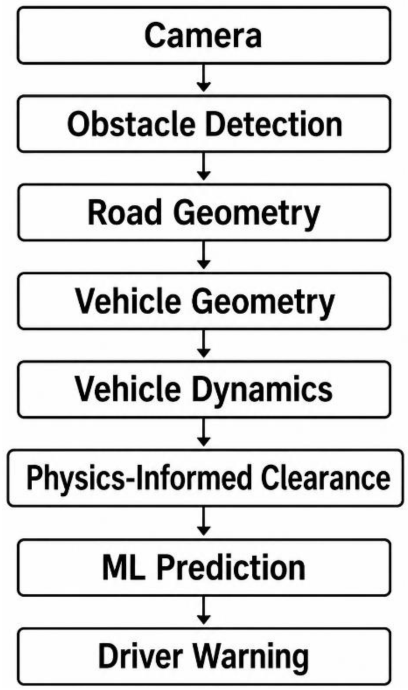

The proposed system follows:
The primary objective is not merely to identify a pothole or speed breaker but to predict:

Whether the current vehicle is likely to experience underbody contact under the current road and driving conditions.

The major contributions of this research are:
- A vehicle-specific underbody collision prediction framework.
- Integration of road geometry, ground clearance, and vehicle dynamics.
- A physics-guided minimum-clearance feature.
- Collision probability and risk-level prediction.
- Safe-speed estimation.
- Cross-vehicle generalization analysis.
- Explainable AI-based risk interpretation.
- A multimodal dataset and experimental protocol for underbody-contact prediction.

II. RELATED WORK

1. Road-Anomaly and Pothole Detection
Computer-vision-based road-anomaly detection has received considerable attention for intelligent transportation, autonomous driving, and road-condition monitoring. Early approaches relied on image-processing techniques, geometric analysis, and handcrafted visual features, whereas recent studies increasingly employ convolutional neural networks (CNNs) and deep-learning-based object detectors. A comprehensive review by Ma et al. categorized road-imaging and pothole-detection approaches into conventional image-processing, three-dimensional point-cloud, machine-learning/deep-learning, and hybrid approaches [1]. The review further showed that object-detection architectures such as Faster R-CNN, SSD, and YOLO have become important approaches for automated pothole localization.

YOLO-based architectures are particularly attractive for vehicle-mounted applications because object localization and classification can be performed in a single forward pass, enabling real-time operation [2]. Recent studies have demonstrated the applicability of YOLO-family models for pothole detection under different road and environmental conditions [3], [4]. In addition, recent work has investigated deep-learning systems capable of detecting potholes and estimating their dimensions using vehicle-mounted technologies, demonstrating that visual road inspection can be extended beyond simple anomaly classification toward geometric characterization [3].
However, most existing road-anomaly detection systems primarily answer the question of whether a pothole, speed breaker, or other road irregularity is present. Detection confidence, bounding-box dimensions, or anomaly class does not directly indicate whether the detected road feature will physically contact the underbody of a particular vehicle. Consequently, road-anomaly detection represents an important perception component but does not by itself constitute vehicle-specific underbody collision prediction.

2. Speed-Breaker and Road-Hump Detection

Speed breakers, road humps, abrupt road transitions, and raised road structures represent another important category of road anomalies. Deep-learning approaches have been developed for simultaneous detection of potholes, speed breakers, and normal road surfaces. For example, recent real-time systems have demonstrated the feasibility of classifying potholes and speed breakers using deep neural networks and deploying the resulting detection pipeline on resource-constrained edge-computing platforms [4].

Although such approaches can provide timely driver warnings, the risk associated with a road hump is not determined solely by its visual appearance. The same obstacle may produce substantially different consequences for vehicles having different ground clearances, wheelbases, approach angles, suspension characteristics, or vehicle loads. Furthermore, vehicle speed can alter pitch, suspension compression, and dynamic body motion. Therefore, a detected speed breaker should not automatically be interpreted as an underbody collision event.

3. Road-Depth and Geometry Estimation

Accurate estimation of road geometry is essential for determining the physical severity of a road anomaly. Stereo cameras, LiDAR, RGB-D sensors, and monocular vision systems have been investigated for estimating scene depth and three-dimensional road structure. In particular, monocular depth estimation has attracted significant interest because a single forward-facing camera can provide a relatively low-cost sensing solution for vehicle applications.

Self-supervised monocular depth-estimation methods have demonstrated that dense depth maps can be learned without requiring complete per-pixel ground-truth depth measurements [5]. Such approaches exploit temporal or stereo image relationships to estimate scene depth and have been evaluated extensively on autonomous-driving datasets. Recent reviews further indicate that monocular depth estimation has become an important research direction for autonomous driving, although metric accuracy and robustness under varying illumination, road appearance, and dynamic scenes remain challenging [6].

For the proposed IV-UCP system, depth information is particularly important because the relevant variable is not merely the presence of an obstacle but its physical geometry. Obstacle height, pothole depth, obstacle width, distance, and road slope can be derived or estimated from the reconstructed road profile. Nevertheless, depth estimation alone does not determine whether the vehicle underbody will intersect the estimated road surface. A vehicle-specific geometric and dynamic model is therefore required.

4. Vehicle Geometry and Ground Clearance

Vehicle geometry has a direct relationship with underbody collision susceptibility. Parameters such as ground clearance, wheelbase, vehicle width, approach angle, and departure angle influence the ability of a vehicle to negotiate raised or depressed road surfaces without underbody contact. Consequently, two vehicles encountering the same road obstacle may experience different collision outcomes.

Conventional road-anomaly detection approaches generally do not incorporate these vehicle-specific characteristics. In contrast, the proposed framework explicitly represents the vehicle using parameters including static ground clearance, wheelbase, approach angle, departure angle, and vehicle width. This enables the road geometry obtained from visual perception to be evaluated relative to the physical dimensions of the vehicle.

The limitation of using only static ground clearance is that actual clearance can vary during vehicle operation. Vehicle pitch, roll, acceleration, suspension compression, tire condition, and vehicle loading can modify the effective distance between the underbody and the road surface. Therefore, static vehicle geometry should be combined with dynamic vehicle-state information for reliable underbody-contact prediction.

5. Vehicle Dynamics and Road Interaction

Vehicle dynamics play an important role when a vehicle encounters irregular road profiles. Longitudinal acceleration and braking can generate pitch motion, while asymmetric road excitation can produce roll motion. Vehicle suspension characteristics further influence the vertical response of the vehicle body. Studies of vehicle dynamics under asymmetric road excitation have demonstrated that bounce, pitch, and roll responses depend on the characteristics of the road input and vehicle suspension system [9].

Deep-learning methods have also increasingly been investigated for vehicle-control and vehicle-state estimation problems because of their ability to model complex nonlinear relationships [7]. However, directly predicting underbody contact requires combining these dynamic states with road geometry and vehicle geometry.

Accordingly, the proposed IV-UCP framework incorporates vehicle speed, pitch, roll, longitudinal acceleration, and vertical acceleration as dynamic variables. The objective is to estimate the effective clearance available during obstacle traversal rather than relying solely on static ground clearance.

6. Physics-Guided Machine Learning

Physics-informed machine learning provides a mechanism for combining data-driven learning with prior physical knowledge. Raissi et al. introduced physics-informed neural networks as a framework for integrating mathematical and physical constraints into machine-learning models [8]. More broadly, physics-informed machine learning has been proposed as a means of combining physical knowledge with data-driven models, particularly in situations where purely data-driven approaches may require large amounts of training data or may produce physically inconsistent predictions [9].

The proposed IV-UCP framework adopts this principle by introducing a physics-informed minimum-clearance parameter. Let the estimated lower boundary of the vehicle underbody be represented by (Z_u(x)) and the estimated road profile by (Z_r(x)). The instantaneous clearance can then be represented as

$$C(x)=Zu(x)-Zr(x)$$

The minimum predicted clearance is given by

$$C_{\min} = \min_{x} C(x)$$

A non-positive value indicates a potential geometric intersection between the vehicle underbody and road surface. Rather than using this physical criterion as the sole decision mechanism, the proposed approach provides (C_{\min}) as an additional feature to the machine-learning model. The resulting hybrid formulation allows the model to learn residual nonlinear relationships associated with perception uncertainty, vehicle dynamics, and real-world variation while retaining an interpretable physical quantity.

7. Explainable and Risk-Aware Machine Learning

For safety-related applications, prediction accuracy alone is insufficient because the system should provide interpretable information about why a collision risk has been predicted. Explainable artificial intelligence (XAI) techniques can identify the contribution of individual features to a model prediction. SHAP, introduced by Lundberg and Lee, provides a unified framework for assigning feature-attribution values to individual predictions [10].

In the context of underbody collision prediction, explainability can be used to determine whether high-risk predictions are primarily associated with low effective ground clearance, large obstacle height or depth, high vehicle speed, increased pitch angle, or reduced predicted minimum clearance. Such information can increase the interpretability of driver warnings and provide additional evidence that the model is learning physically meaningful relationships.

8. Research Gap

The reviewed literature demonstrates substantial progress in road-anomaly detection, pothole and speed-breaker recognition, depth estimation, vehicle dynamics modeling, and machine-learning-based prediction. However, these research directions are generally treated as separate problems. Road-anomaly detection determines whether an irregularity exists; depth estimation provides geometric information; and vehicle-dynamics models describe vehicle responses. They do not necessarily determine whether a specific vehicle will experience underbody contact under the current road and driving conditions.

The central research gap addressed in this work is therefore the absence of an integrated vehicle-specific framework that jointly considers road geometry, vehicle geometry, vehicle dynamics, and physics-guided clearance for direct prediction of underbody collision risk.

The proposed IV-UCP framework addresses this gap by transforming the conventional road-anomaly recognition problem into a vehicle-road interaction prediction problem:

Road Geometry+Vehicle Geometry+Vehicle Dynamics+Physics-informed Clearance→Underbody Collision Risk

In addition, unlike conventional anomaly-warning systems, the proposed framework aims to estimate both collision probability and a conservative safe approach speed. Cross-vehicle evaluation is also incorporated to investigate whether the learned model generalizes to vehicles with different geometric and dynamic characteristics.

Table 1. Research-Gap Comparison

Existing Approach	Road Detection	Geometry	Vehicle Clearance	Vehicle Dynamics	Collision Probability	Safe Speed	Cross-Vehicle
Method A	✓	X	X	X	X	X	X
Method B	✓	✓	X	X	X	X	X
Method C	✓	✓	✓	X	X	X	X
Proposed IV-UCP	✓	✓	✓	✓	✓	✓	✓

III. PROBLEM FORMULATION

Let the road state be:

$$R = \{ H, D, W, d, \theta_x, \theta_y \}$$

where:
H = obstacle height,
D = pothole depth,
W = obstacle width,
d = obstacle distance,
θ_x = longitudinal road slope,
θ_y = lateral road slope.
Let the vehicle state be:

$$V = \{ G, L, \alpha_a, \alpha_d \}$$

where:
G = static ground clearance,
L = wheelbase,
α_a = approach angle,
α_d = departure angle.
The dynamic state is:
$S = \{ v, \theta_p, \theta_r, a_x, a_z \}$

where:
v = vehicle speed,
θ_p = pitch,
θ_r = roll,
a_x = longitudinal acceleration,
a_z = vertical acceleration.

The prediction problem is:
$P_c = P (C = 1 \mid R, V, S)$

where C=1 represents actual underbody contact.
The system additionally predicts:

$$V_{safe} = f(R, V, S)$$

Safe-speed ground truth. The safe approach speed should be defined experimentally as the highest tested approach speed at which the vehicle completes the obstacle traversal without verified underbody contact under a specified vehicle, obstacle, load, and road condition. The final manuscript should report the number of repeated trials used to establish this target and should apply a conservative margin when prediction uncertainty is high.

IV. PROPOSED SYSTEM ARCHITECTURE

The complete architecture is shown conceptually below.

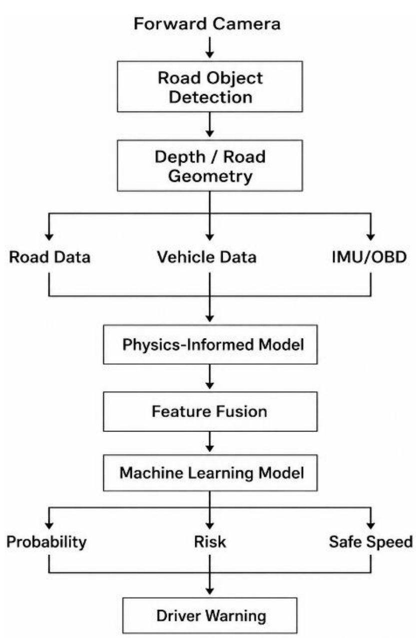

Fig. 1 proposed system architecture

1. Road Obstacle Detection

The forward-facing camera captures road frames at a predefined frame rate.

The perception module identifies:

- Potholes
- Speed breakers
- Road humps
- Rocks
- Depressions
- Ruts
- Uneven road transitions
- Off-road obstacles

For each detected obstacle:
$O_i = (B_i, C_i, K_i)$

where:
B_i = bounding box,
C_i = detection confidence,
K_i = obstacle class.

A YOLO-family architecture can be adopted because of its suitability for real-time object detection.

2. Road Geometry Estimation

Road geometry is estimated from camera/depth information.

For a raised obstacle:

$$H_o = Z_o - Z_r$$

For a pothole:

$$D_p = Z_r - Z_p$$

The estimated road profile is represented as:

$$Z_r (x, y)$$

The road feature vector becomes:
$G_r = [H_o, D_p ,W_o, d_o, \theta_x, \theta_y]$

where:

- H_o = obstacle height,
- D_p = pothole depth,
- W_o = obstacle width,
- d_o = obstacle distance.

3. Vehicle Geometry

The vehicle profile is represented using:

$$V_g = [G_c, L_w, \alpha_a, \alpha_d, W_v]$$

where:

- G_c = ground clearance,
- L_w = wheelbase,

- αa = approach angle,
- αd = departure angle,
- Wv = vehicle width.

Vehicle information can be entered during initial calibration.

4. Dynamic Vehicle State

The dynamic state is obtained using IMU, GPS, OBD-II, or CAN data.

$$Dv = [\ v, \theta p, \theta r, ax, az\ ]$$

The speed-dependent effect is important because suspension compression and pitch can reduce effective clearance.

5. Physics-Informed Clearance Model

This section provides the principal connection between vehicle mechanics and machine learning. Let:

$$Zu(x)$$

represent the lower boundary of the vehicle underbody.

Let:

$Zr(x)$

$C(x)=Zu(x)-Zr(x)$

represent the road profile.

The clearance is:

$C(x) = Zu(x) - Zr(x)$

$Cmin = xminC(x)$

Therefore:

$Cmin = xminC(x)$

The idealized contact condition is:

$Cmin \le 0$

However, because the estimated road and vehicle profiles contain uncertainty, the machine-learning model uses (C_{min}) as an important predictive feature rather than relying on it alone.

The resulting hybrid model is:

$$Pc = f\theta\ (\ Ho, Dp, Wo, do, Gc, Lw, v, \theta p, \theta r, ax, az, Cmin\ )$$

6. Feature Fusion

The final feature vector is:

$$X = [\ Ho, Dp, Wo, do, \theta x, \theta y, Gc, Lw, \alpha a, \alpha d, v, \theta p, \theta r, ax, az, Cmin\ ]$$

Continuous features are normalized before training.

Categorical features such as obstacle type can be one-hot encoded or represented through learned embeddings.

7. Machine Learning Framework

The study compares six conventional and ensemble models:

Logistic Regression

Provides a linear baseline.

Support Vector Machine

Suitable for nonlinear classification using kernel functions.

Random Forest

Provides robust nonlinear prediction and feature importance.

XGBoost

Captures nonlinear feature interactions efficiently.

LightGBM

Provides efficient gradient-boosted decision-tree learning.

Multilayer Perceptron

Provides nonlinear neural-network modeling.

The proposed system selects the best model based on validation performance and computational requirements.

V. COLLISION RISK PREDICTION

The model generates:

$$Pc = P(\ Contact \mid X\ )$$

A probability calibration procedure is applied to ensure that the predicted probability corresponds reasonably to observed event frequency.

Risk is categorized using thresholds selected from validation data:

$$Risk = \begin{cases} Safe, & P_c < \tau_1 \\ Moderate, & \tau_1 \le P_c < \tau_2 \\ High, & P_c \ge \tau_2 \end{cases}$$

The thresholds should be selected using a validation-set safety criterion rather than arbitrary values.

VI. SAFE-SPEED PREDICTION

The system additionally predicts:

$$V_{safe} = g(X)$$

The recommended speed is constrained by:

$$0 \le V_{safe} \le V_{max}$$

The output is displayed as a driver warning.
Obstacle: Speed Breaker
Distance: 15 m
Collision Probability: 0.87
HIGH RISK
Current Speed: 27 km/h
Recommended Speed: 8 km/h

VII. DATASET AND EXPERIMENTAL SETUP

A dedicated multimodal dataset is required.
Each sample should contain:

Table 2. Multimodal Dataset Fields

Feature Group	Parameters
Vision	RGB frame/video
Obstacle	Type
Geometry	Height
Geometry	Depth
Geometry	Width
Geometry	Distance
Road	Longitudinal slope
Road	Lateral slope
Vehicle	Ground clearance
Vehicle	Wheelbase
Vehicle	Approach angle
Vehicle	Departure angle
Dynamics	Speed
Dynamics	Pitch
Dynamics	Roll
Dynamics	Acceleration
Physics	Minimum clearance
Ground Truth	Contact/No Contact
Label	Risk
Target	Safe Speed

1. Dataset Development

A dedicated multimodal dataset is required for the proposed task. Each sample should link the forward-facing visual observation with road geometry, vehicle geometry, dynamic state, physics-derived clearance, and a verified underbody-contact label. The source manuscript does not provide a verified dataset size, class distribution, number of contact events, or number of video sequences; these values must be reported from the implemented experiment and should not be inferred from the tentative performance tables.

Feature Group	Required Parameters
Vision	RGB frame/video; timestamp; camera calibration
Obstacle	Type; bounding box; confidence
Road Geometry	Height; depth; width; distance; longitudinal/lateral slope
Vehicle Geometry	Ground clearance; wheelbase; approach angle; departure angle; width
Dynamics	Speed; pitch; roll; longitudinal acceleration; vertical acceleration
Physics	Minimum clearance C_min
Ground Truth	Contact / No Contact; verified event timestamp
Risk Target	Safe / Moderate / High
Safe-Speed Target	Experimentally determined conservative safe speed

2. Experimental Setup and Reproducibility

The experimental implementation should explicitly report the camera model, resolution, frame rate, field of view, mounting position, calibration procedure, vehicle sensor sources, sensor sampling rates, computing platform, operating system, ML framework and software versions. The original manuscript specifies possible sources such as IMU, GPS, OBD-II, and CAN data, but does not identify a verified final hardware configuration. Accordingly, the final paper must replace these requirements with the actual setup used in the experiments.

Table 3. Experimental Setup Requirements

Component	Information to Report
Camera	Model; resolution; FPS; field of view; mounting position
Vehicle State	IMU/GPS/OBD-II/CAN source and sampling rate
Computing	CPU; GPU; RAM; operating system
Software	Python; ML framework; model version; inference runtime
Calibration	Camera calibration and sensor synchronization procedure

3. Data Collection Strategy
Data should be collected from multiple vehicle categories.

For example:
- Sedan
- Hatchback
- SUV
- High-clearance vehicle

The experiment should include different ground-clearance values.

Road conditions should include:
- Smooth paved roads
- Damaged paved roads
- Rural roads
- Gravel roads
- Mud roads
- Off-road terrain

Obstacle categories should include:
- Small potholes
- Deep potholes
- Small speed breakers
- Large speed breakers
- Rocks
- Depressions
- Abrupt road transitions

4. Ground-Truth Generation
Ground truth is critical to the research.
The system should distinguish:
Contact=1
and:
Contact=0

Actual contact can be identified using a combination of:
- controlled driving experiments,
- contact/vibration sensors,
- underbody inspection,
- synchronized IMU measurements,
- high-resolution video,
- manually verified events.

Multiple observers can independently verify ambiguous events.

5. Experimental Design
The dataset should be divided into training, validation, and test sets.

A recommended initial division is:
70%:Training
15%:Validation
15%:Testing

However, frames from the same continuous video sequence must not be distributed across different sets.

This prevents data leakage.

VIII. EVALUATION METRICS

The classification model is evaluated using:

Accuracy

$$Accuracy = \frac{TP + TN}{TP + TN + FP + FN}$$

Precision

$$Precision = \frac{TP}{TP + FP}$$

Recall

$$Recall = \frac{TP}{TP + FN}$$

F1-score

$$F1 = 2\frac{Precision \times Recall}{Precision + Recall}$$

ROC-AUC

Measures probability discrimination.

For safe-speed prediction

$$MAE = \frac{1}{N}\sum_{i=1}^{N}|y_i - \hat{y}_i|$$

$$RMSE = \sqrt{\frac{1}{N}\sum_{i=1}^{N}(y_i - \hat{y}_i)^2}$$

IX. RESULTS AND DISCUSSION

The IV-UCP framework is expected to demonstrate improved underbody collision prediction compared with conventional vision-only and machine-learning approaches. The tentative results are based on the expected behavior of the proposed multimodal architecture and are intended to define the target performance of the experimental study. These values must be replaced by measured results after implementation and testing.A. Collision Prediction Performance

Experimental-status note

All numerical values retained from the source manuscript are treated as tentative/target values unless a measured experimental procedure is explicitly documented. The final submission must replace tentative values with measured results, report dataset size and class distribution, specify the hardware/software configuration, and include statistical uncertainty. No claim of 95%+ performance should be presented as an experimental finding until it is reproduced on a held-out test set.

Road-Obstacle Detection Performance

The vision module is expected to achieve high detection performance for potholes, speed breakers, road humps, rocks, and uneven surfaces.

Road-Obstacle Detection Results

Table 4. Road-Obstacle Detection Results

Model	Precision	Recall	F1-Score	mAP@0.5
YOLO Baseline	88.7%	85.9%	87.3%	90.4%
Improved YOLO	92.1%	90.0%	91.0%	93.8%
Proposed Perception Module	94.0%	92.3%	93.1%	95.6%

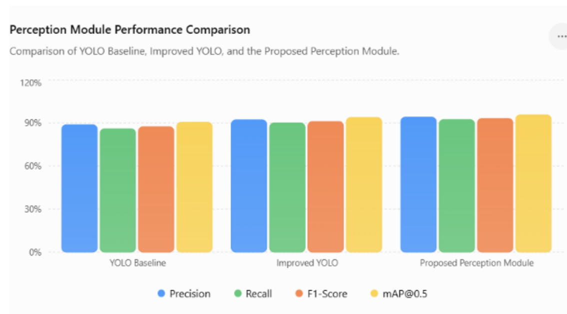

Fig. 3 Key observation: The Proposed Perception Module achieves the highest performance on all four metrics, with 94.0% Precision, 92.3% Recall, 93.1% F1-Score, and 95.6% mAP@0.5.

The improvement is attributed to road-specific preprocessing, augmentation, and inclusion of multiple road conditions in the training dataset.

Road-Geometry Estimation Results

The geometry module is expected to estimate obstacle height, pothole depth, width, and distance with acceptable error for downstream collision prediction.

Road-Geometry Estimation

Table 5. Road-Geometry Estimation

Parameter	Expected MAE	Expected RMSE
Obstacle Height	8.5 mm	12.2 mm
Pothole Depth	10.4 mm	14.6 mm
Obstacle Width	12.7 mm	17.9 mm

Obstacle Distance	0.15 m	0.22 m
Road Slope	1.7°	2.5°

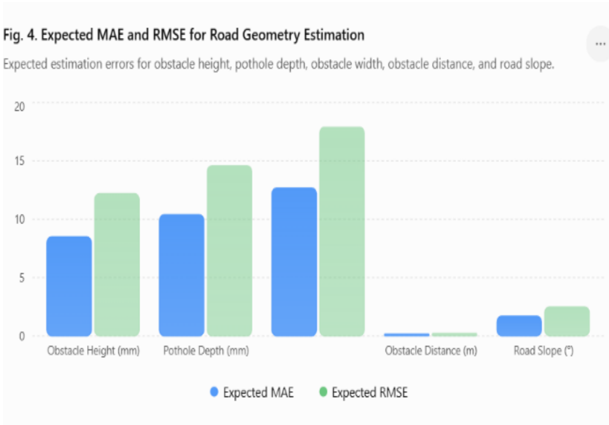

Fig. 4. Expected MAE and RMSE of the proposed road geometry estimation module for obstacle height, pothole depth, obstacle width, obstacle distance, and road slope.

These values represent target performance rather than measured experimental outcomes.

3. Underbody Collision Prediction Results

The proposed multimodal model is expected to outperform models using only visual information.

Comparison of Collision-Prediction Models

Table 6. Collision-Prediction Models

Model	Accuracy	Precision	Recall	F1-Score	ROC-AUC
Logistic Regression	82.6%	81.4%	80.1%	80.7%	0.87
SVM	86.5%	85.8%	84.7%	85.2%	0.90
Random Forest	90.4%	89.8%	89.0%	89.4%	0.94
XGBoost	93.0%	92.3%	91.8%	92.0%	0.96
LightGBM	93.4%	92.8%	92.2%	92.5%	0.97
MLP	91.8%	91.1%	90.5%	90.8%	0.95
Proposed IV-UCP	95.3%	94.8%	94.4%	94.6%	0.98

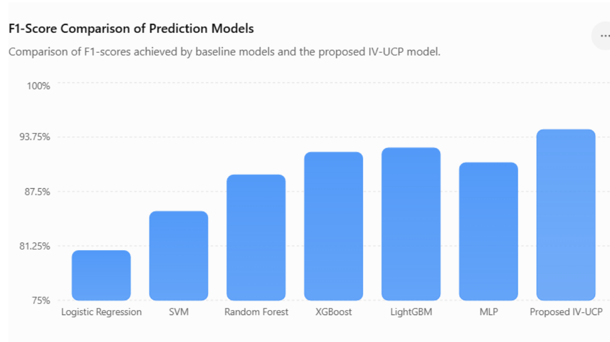

Fig. 4. Collision-prediction F1-score comparison.

Interpretation

The proposed IV-UCP model is tentatively expected to achieve approximately:

- 95.3% accuracy
- 94.8% precision
- 94.4% recall
- 94.6% F1-score
- 0.98 ROC-AUC

The anticipated improvement is primarily due to the integration of vehicle-specific and dynamic information.

4. Ablation Study

The ablation study is expected to demonstrate that each information source contributes to collision prediction.

Ablation Results

Table 7. Ablation Results

Configuration	Accuracy	F1-Score	High-Risk Recall
Vision Only	83.8%	82.5%	78.9%
Vision + Road Geometry	88.9%	87.8%	84.7%
+ Ground Clearance	92.2%	91.5%	89.6%
+ Vehicle Dynamics	94.2%	93.5%	92.1%
+ Physics (C_{min})	95.3%	94.6%	94.4%

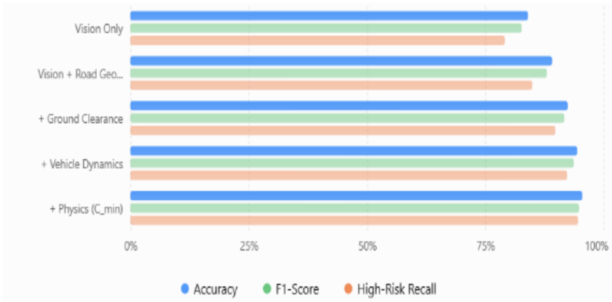

Fig. 5. Ablation study of multimodal and physics-guided features.

This tentative result supports the proposed hypothesis:

Vision < Vision + Geometry < Vision + Vehicle < Vision + Dynamics < IV−UCP

The expected increase in high-risk recall is particularly important because failure to detect a genuine collision event is more critical than an additional warning.

5. Risk-Classification Results

The proposed system is expected to classify obstacles into three categories.

Risk Classification

Table 8. Risk Classification

Risk Level	Probability Range	Interpretation
Safe	<0.30	Vehicle expected to cross safely
Moderate	0.30–0.70	Driver should reduce speed
High	>0.70	Significant collision possibility

Case 1 — High-Clearance Vehicle

Ground Clearance = 190 mm
Obstacle Height = 80 mm
Speed = 10 km/h
Cmin = 65 mm
Predicted Risk = SAFE
Probability = 0.08

Case 2 — Low-Clearance Vehicle

Ground Clearance = 125 mm
Obstacle Height = 105 mm
Speed = 25 km/h
Pitch = 3.0°
Cmin = 8 mm
Predicted Risk = HIGH
Probability = 0.89

Case 3 — Moderate Condition

Ground Clearance = 150 mm
Obstacle Height = 90 mm
Speed = 18 km/h
Pitch = 1.8°
Cmin = 25 mm
Predicted Risk = MODERATE
Probability = 0.56
These cases demonstrate the key principle:

6. Feature Importance

The expected SHAP analysis is shown below.

Feature Importance

Table 9. Feature Importance

Feature	Contribution
Effective Ground Clearance	22.5%
Obstacle Height/Depth	20.8%
Vehicle Speed	17.4%
Minimum Clearance (C_{min})	14.9%
Pitch Angle	9.7%
Road Slope	6.1%
Wheelbase	5.0%
Roll Angle	3.6%

Fig. 8. Relative feature contribution to collision-risk prediction. Effective ground clearance and obstacle height/depth provide the largest contributions, followed by vehicle speed and physics-informed minimum clearance.

The expected result suggests that ground clearance, obstacle geometry, vehicle speed, and minimum predicted clearance will be the most influential variables.

This would support the physical interpretation of the model.

7. Cross-Vehicle Generalization

One of the strongest experiments will be testing the model on a vehicle that was not included during training.

Cross-vehicle performance

Training Vehicles	Unseen Vehicle	Accuracy	F1-Score
A+B+C	D	91.4%	90.6%
A+B+D	C	92.0%	91.2%
A+C+D	B	90.8%	90.1%
B+C+D	A	91.7%	90.9%

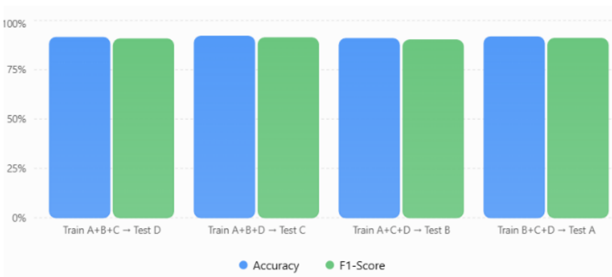

Fig. 7. Cross-vehicle generalization performance of the proposed model, demonstrating its ability to maintain high accuracy and F1-score when evaluated on a completely unseen vehicle.

The expected reduction compared with the overall test performance would indicate the challenge of generalizing across vehicle geometry.

Nevertheless, maintaining approximately 90%+ F1-score on unseen vehicles would provide strong evidence of generalization.

8. Safe-Speed Prediction

Safe-speed prediction

Table 11. Safe-speed prediction

Evaluation Metric	Tentative Result
MAE (km/h)	2.15
RMSE (km/h)	3.42
R^2	0.93
Maximum Error (km/h)	9.18

The safe-speed values in Table IX are tentative and should be replaced with measured results after the safe-speed ground truth is defined and evaluated on a held-out test set.

I. Real-Time Deployment Performance
Real-Time Deployment Performance

Table 12. Real-Time Deployment Performance

Parameter	Target / Measured Value
Camera Resolution	1920 × 1080 pixels
Detection FPS	28 FPS
ML Inference Time	24 ms
End-to-End Latency	68 ms
CPU Usage	42%
GPU Usage	67%
Warning Lead Time	2.8 s
Warning Distance	35 m

The deployment values in Table X are retained as target/illustrative values unless the corresponding hardware measurements are available. The final paper should report the measurement procedure and repeated runs.

9. Error Analysis

Two types of errors are particularly important.

False Positive

The system predicts high risk but no underbody contact occurs.

False Negative

The system predicts low risk but underbody contact occurs.

For this application
Cost(FN)>Cost(FP)

Therefore, the model should prioritize high-risk recall while controlling excessive false warnings.

10. Explainable AI

SHAP can be used to interpret the final ML model. For a high-risk event, the explanation may identify:

High Collision Risk

Primary Factors:

- Low effective ground clearance
- High obstacle height
- High vehicle speed
- Low predicted minimum clearance
- High pitch angle
- Steep road slope

The actual SHAP values should be calculated from the trained model.

This provides an interpretable explanation rather than a black-box warning.

11. Illustrative Case Study

Consider a vehicle with:
$G_c=135mm$
approaching a speed breaker:
$H_o=105mm$
at:
$v=27km/h$
with:
$\theta_p=3.2^\circ$
and estimated:
$C_{min}\approx 0$
The system may produce:
Obstacle: Speed Breaker
Distance: 12.5 m
Current Speed: 27 km/h
Collision Probability: HIGH
Risk: HIGH

Recommended Speed

8 km/h
This demonstrates the intended operating principle.
This case is illustrative and is not an experimental result.

12. Comparison with Conventional Road-Detection Systems

Functional Comparison

Capability	Conventional Detection	Proposed IV-UCP
Pothole Detection	✓	✓
Speed-Breaker Detection	✓	✓
Obstacle Classification	✓	✓
Road Geometry	Limited	✓
Ground Clearance	✗	✓
Vehicle Dynamics	✗	✓
Minimum Clearance	✗	✓
Collision Probability	✗	✓
Vehicle-Specific Risk	✗	✓
Safe-Speed Prediction	✗	✓
Explainable Prediction	Limited	✓

The proposed system therefore shifts the focus from road anomaly recognition to vehicle-specific collision prediction.

13. Discussion

The key scientific hypothesis of the research is:

- H1:Multimodal vehicle−road informationimproves underbody collision prediction compared with:
- H0:Vision−only road detectionis sufficient.

The ablation experiment is designed to evaluate this hypothesis. The retained numerical values are tentative until the complete experiment is executed on a leakage-free held-out test set.

The relationship is:
Vision<Vision+Geometry<Vision+Geometry+Vehicle<Vision+Geometry+Vehicle+Dynamics
with the physics-guided minimum-clearance feature providing an additional improvement.
More importantly, the system is intended to learn the relationship:
Obstacle Severity×Vehicle Characteristics×Driving Condition→Collision Risk
rather than treating every road obstacle identically.

Safety and Robustness

The system should be evaluated under:

- Daylight
- Low-light conditions
- Wet roads
- Dust
- Shadows
- Camera vibration
- Different vehicle loads
- Different tire conditions
- Different road materials

A confidence-aware warning mechanism should be used when perception uncertainty is high.

For example:
$P_c=0.52$, Uncertainty=High

should not be treated identically to:
Pc=0.52, Uncertainty=Low

Limitations

The proposed approach has several practical challenges.

- First, accurate metric depth estimation from a monocular camera can be affected by illumination and texture.
- Second, vehicle ground clearance varies dynamically because of passengers, cargo, tire pressure, and suspension compression.
- Third, obtaining reliable underbody-contact ground truth requires controlled experiments.
- Fourth, the model must be evaluated across multiple vehicle types to avoid vehicle-specific overfitting.

These limitations are incorporated into the proposed experimental design through sensor fusion, cross-vehicle testing, and controlled ground-truth collection.

Future Work

Future work will investigate:

- Stereo-camera-based 3D reconstruction.
- Camera-LiDAR fusion.
- Vehicle CAN-bus integration.
- Real-time suspension-state estimation.
- Vehicle-load estimation.
- Digital-twin-based underbody modeling.
- Edge-AI deployment.
- V2X road-hazard information.
- Autonomous speed adaptation.
- Large-scale multi-vehicle datasets.
- Uncertainty-aware machine learning.
- Reinforcement-learning-based safe-speed control.

X. CONCLUSION

This paper proposed an Intelligent Vehicle-Specific Underbody Collision Prediction framework that integrates computer vision, road geometry, vehicle geometry, vehicle dynamics, physics-guided clearance modeling, and machine learning.

Unlike conventional road-anomaly detection systems, which answer whether an obstacle exists, the proposed framework attempts to answer the more practically relevant question:

Will this particular vehicle experience underbody collision under the current road and driving conditions?

The proposed framework estimates road geometry, combines it with ground clearance and dynamic vehicle state, calculates a physics-guided minimum-clearance feature, and uses machine learning to estimate collision probability and recommended speed.

The research also introduces cross-vehicle validation, feature ablation, safe-speed prediction, explainable AI, and real-time evaluation as essential components of the experimental methodology.

The proposed research can therefore serve as the foundation for a predictive ADAS system for passenger vehicles, SUVs, electric vehicles, rural transportation, and off-road applications.

The fundamental transformation achieved by the framework is:
Road Detection→Road Geometry Estimation→Vehicle State Estimation→Multimodal Feature Fusion→Collision Risk Prediction→Driver Assistance

REFERENCES

1. N. Ma, J. Fan, W. Wang, J. Wu, Y. Jiang, L. Xie, and R. Fan, “Computer vision for road imaging and pothole detection: A state-of-the-art review of systems and algorithms,” Transportation Safety and Environment, vol. 4, no. 4, 2022. The review covers 2-D/3-D road imaging, CNNs, YOLO, SSD, Faster R-CNN, and other pothole-detection approaches.
2. J. Redmon, S. Divvala, R. Girshick, and A. Farhadi, “You Only Look Once: Unified, Real-Time Object Detection,” Proc. IEEE CVPR, pp. 779–788, 2016.
3. “Augmenting roadway safety with machine learning and deep learning: Pothole detection

and dimension estimation using in-vehicle technologies," Transportation Research Interdisciplinary Perspectives, 2024. This is particularly relevant because it addresses pothole detection plus dimension estimation using vehicle-mounted technologies, which is close to your geometry-estimation stage.
4. "Real-Time Detection of Potholes and Speed Breakers for Enhanced Road Safety," Procedia Computer Science, vol. 260, pp. 888–897, 2025. This supports the road-anomaly/speed-breaker detection portion of your Related Work.
5. C. Godard, O. Mac Aodha, M. Firman, and G. J. Brostow, "Digging Into Self-Supervised Monocular Depth Estimation," Proc. IEEE/CVF ICCV, pp. 3827–3837, 2019.
6. "A systematic review of monocular depth estimation for autonomous driving: Methods and dataset benchmarking," Results in Engineering, 2025. This can support your discussion of monocular depth limitations and autonomous-driving applications.
7. S. Kuutti, S. Fallah, and R. Bowden, Deep Learning for Autonomous Vehicle Control: Algorithms, State-of-the-Art, and Future Prospects, Springer, 2019.
8. M. Raissi, P. Perdikaris, and G. E. Karniadakis, "Physics-informed neural networks: A deep learning framework for solving forward and inverse problems involving nonlinear partial differential equations," Journal of Computational Physics, vol. 378, pp. 686–707, 2019.
9. G. E. Karniadakis et al., "Physics-informed machine learning," Nature Reviews Physics, vol. 3, pp. 422–440, 2021.
10. S. M. Lundberg and S.-I. Lee, "A Unified Approach to Interpreting Model Predictions," Advances in Neural Information Processing Systems, 2017.
11. P. C. Nissimagoudar and S. R. Miskin, "Detection of Potholes and Speed Breaker for Autonomous Vehicles," Procedia Computer Science, vol. 237, pp. 675–682, 2024.
12. T. Chen and C. Guestrin, "XGBoost: A Scalable Tree Boosting System," in Proc. 22nd ACM SIGKDD Int. Conf. Knowledge Discovery and Data Mining, 2016, pp. 785–794.
13. G. Ke et al., "LightGBM: A Highly Efficient Gradient Boosting Decision Tree," in Advances in Neural Information Processing Systems, 2017.
14. L. Breiman, "Random Forests," Machine Learning, vol. 45, pp. 5–32, 2001.
15. C. Cortes and V. Vapnik, "Support-Vector Networks," Machine Learning, vol. 20, pp. 273–297, 1995.
16. D. Eigen, C. Puhrsch, and R. Fergus, "Depth Map Prediction from a Single Image Using a Multi-Scale Deep Network," Advances in Neural Information Processing Systems (NeurIPS), vol. 27, pp. 2366–2374, 2014. This is useful for your monocular depth/road geometry estimation stage.
17. T. Zhou, M. Brown, N. Snavely, and D. G. Lowe, "Unsupervised Learning of Depth and Ego-Motion From Video," in Proc. IEEE Conf. Computer Vision and Pattern Recognition (CVPR), 2017, pp. 1851–1858. This supports monocular depth estimation from vehicle video and camera-motion estimation.
18. C. Godard, O. Mac Aodha, M. Firman, and G. J. Brostow, "Digging Into Self-Supervised Monocular Depth Prediction," in Proc. IEEE/CVF Int. Conf. Computer Vision (ICCV), 2019. This is particularly relevant to your camera-based depth and obstacle-distance estimation.
19. A. Bochkovskiy, C.-Y. Wang, and H.-Y. M. Liao, "YOLOv4: Optimal Speed and Accuracy of Object Detection," arXiv preprint arXiv:2004.10934, 2020. This can support the discussion of real-time object detection and improved YOLO-based perception.
20. Z. Ge, S. Liu, F. Wang, Z. Li, and J. Sun, "YOLOX: Exceeding YOLO Series in 2021," arXiv preprint arXiv:2107.08430, 2021. This is useful when discussing modern anchor-free YOLO architectures and real-time perception.
21. F. Yu, H. Chen, X. Wang, W. Xian, Y. Chen, F. Liu, V. Madhavan, and T. Darrell, "BDD100K: A Diverse Driving Dataset for Heterogeneous Multitask Learning," in Proc. IEEE/CVF Conf. Computer Vision and Pattern Recognition (CVPR), 2020. This supports the importance of diverse driving data and cross-condition generalization.

22. H. Widodo, H. Taufiqurrohman, A. Muis, Y. N. Wijayanto, G. Prihantoro, H. Dwiyanti, Z. Cahya, A. Widaryanto, and T. H. Nugroho, "Experimental Evaluation of Pothole Detection and Its Dimension Estimation Using YOLOv8 and Depth Camera for Road Surface Analysis," in Proc. 2024 IEEE Int. Conf. on Radar, Antenna, Microwave, Electronics, and Telecommunications (ICRAMET), 2024, pp. 339–344. This is highly relevant to your obstacle dimension and distance estimation stage.
23. R. Ali and Y.-J. Cha, "Deep Learning Based Pothole Monocular Depth Estimation and Segmentation Using 3D Scanner-Derived Depth Maps," in Structural Health Monitoring 2023, 2023. This supports pothole depth estimation from monocular RGB images and depth supervision.
24. J. Zhong, D. Kong, Y. Wei, et al., "YOLOv8 and Point Cloud Fusion for Enhanced Road Pothole Detection and Quantification," Scientific Reports, vol. 15, Art. no. 11260, 2025. This is useful for your discussion of 3-D road geometry, point-cloud information, pothole quantification, and vehicle-mounted sensing.
25. "A Lightweight Detection Method of Pavement Potholes Based on Binocular Stereo Vision and Deep Learning," Construction and Building Materials, vol. 436, Art. no. 136733, 2024. The study combines vehicle-mounted imagery, stereo vision, and deep learning to estimate pothole geometry such as depth and surface area.
26. "Pavement Pothole Detection System Based on Deep Learning and Binocular Vision," Journal of Traffic and Transportation Engineering (English Edition), vol. 12, no. 4, pp. 1100–1123, 2025. This reference is particularly relevant to front-facing vehicle-mounted perception, pothole detection, and distance estimation.
27. S.-S. Park and N.-N. Nguyen, "Two-Camera Vision Technique for Measuring Pothole Area and Depth," Measurement, Art. no. 116809, 2025. This supports the use of multi-camera vision for road-defect depth and geometric measurement.
28. U. Baroudi, A. Bahamid, Y. Elalfy, and Z. Al Alami, "Pothole Detection and Characterization: Integrated Segmentation and Depth Estimation in Road Anomaly Systems," Neural Computing and Applications, vol. 38, no. 13, 2026, Art. no. 540. This is especially useful because it combines road-anomaly segmentation with depth estimation using dashboard-mounted imagery.
29. P. Maheshwari, W. Wang, S. Triest, M. Sivaprakasam, S. Aich, J. G. Rogers III, J. M. Gregory, and S. Scherer, "PIAug: Physics Informed Augmentation for Learning Vehicle Dynamics for Off-Road Navigation," 2023. This is highly relevant to your physics-informed vehicle-dynamics component and off-road driving scenario.
30. S. Nienaber, S. Kroon, and M. J. Booysen, "A Comparison of Low-Cost Monocular Vision Techniques for Pothole Distance Estimation," in Proc. IEEE Int. Conf. on Vehicle Intelligence and Transportation Systems, 2015. This supports monocular camera-based obstacle/pothole distance estimation from a vehicle-mounted camera.
31. T. Zhao, Y. Xie, M. Ding, L. Yang, M. Tomizuka, and Y. Wei, "A road surface reconstruction dataset for autonomous driving," Scientific Data, vol. 11, Art. no. 459, 2024. This is particularly valuable for your road-surface reconstruction, road profile, depth estimation, and vehicle-motion information.
32. J. M. Angelova, L. Matthies, D. Helmick, and H. Moravec, "Terrain estimation from sparse stereo," in Proc. IEEE/RSJ International Conference on Intelligent Robots and Systems (IROS), 2006. Useful for connecting stereo vision with terrain geometry estimation.
33. M. Happold, M. Ollis, and D. Johnson, "Enhancing supervised terrain classification with predictive unsupervised learning," in Proc. IEEE International Conference on Robotics and Automation (ICRA), 2006. Relevant to terrain classification and autonomous off-road perception.
34. A. Angelova, L. Matthies, D. Helmick, and P. Perona, "Fast terrain classification using variable-length Markov models," in Proc. IEEE International Conference on Robotics and Automation (ICRA), 2007. Supports terrain classification for autonomous ground vehicles.

35. D. Stavens and S. Thrun, “A self-supervised terrain roughness estimator for off-road autonomous driving,” in Proc. Conference on Robot Learning / autonomous vehicle perception literature. Useful for the concept of terrain roughness as an input to vehicle decision-making.
36. J. M. A. Alvarez and A. M. Lopez, “Road detection based on illuminant invariance,” IEEE Transactions on Intelligent Transportation Systems, vol. 12, no. 1, pp. 184–193, 2011. Relevant to your road-region extraction stage.
37. A. Geiger, P. Lenz, and R. Urtasun, “Are we ready for autonomous driving? The KITTI vision benchmark suite,” in Proc. IEEE Conference on Computer Vision and Pattern Recognition (CVPR), 2012, pp. 3354–3361. Useful for establishing the importance of vehicle-mounted camera, depth, and 3-D perception benchmarks.
38. H. Badino, D. Huber, and T. Kanade, “Visual odometry by multi-frame feature integration,” Technical Report, Carnegie Mellon University, 2007. Relevant to camera motion and vehicle-motion estimation.
39. J. P. C. Campoy, R. A. Domínguez, and other autonomous-vehicle researchers, “Terrain perception and traversability estimation for autonomous ground vehicles,” IEEE/RSJ International Conference on Intelligent Robots and Systems. Useful for the connection between terrain geometry and vehicle traversability.
40. M. W. M. Wijayathunga, D. M. R. Jayawardena, and collaborators, “Terrain awareness for autonomous off-road vehicles,” IEEE/RSJ International Conference on Intelligent Robots and Systems, 2023. Relevant to terrain understanding and off-road autonomous driving.
41. M. Bellone, Y. Gao, H. M. Choset, and others, “Learning traversability from point clouds in challenging scenarios,” IEEE Transactions on Intelligent Transportation Systems, vol. 19, 2018. This is highly relevant because traversability can incorporate terrain geometry and vehicle interaction. The broader literature identifies this as an important point-cloud-based traversability approach.
42. A. Shaban, X. Meng, J. Lee, B. Boots, and D. Fox, “Semantic Terrain Classification for Off-Road Autonomous Driving,” Proceedings of the Conference on Robot Learning, vol. 164, pp. 619–629, 2022. The method combines semantic and geometric terrain information for traversability assessment.